Effect of Microstructure on Hydride Precipitation in Ti-6A1-4V Alloy †

Toshio ENJO* and Toshio KURODA**

Abstract

Effect of the microstructure on the hydride precipitation behavior has been studied on a Ti-6Al-4V alloy cathodically charged at various current densities using internal friction measurement and transmission electron microscopy.

The hydride precipitation by cathodic charging was observed not only near the surface but also inside the specimen for the β annealed specimen consisting of α + β microstructure. The γ hydride precipitation was observed only near the surface of the specimen for the β quenched specimen of α′ microstructure, and for the α + β quenched specimen consisting of α + α′ microstructure. The γ hydride phase precipitated at the α/β interface and inside the α and β phases for the β annealed specimen. The γ phase also precipitated at the α/β or α′/α interface and inside the α′ phase for the α + β quenched specimen.

An internal friction peak appearing at 190–220 K by using 1 Hz was related to hydride precipitation. The peak height increased with increasing cathodic charging time.

The precipitation of hydrides caused the Bordoni peak related to the strain of α phase matrix. The peak at 220–280 K at 1 Hz appeared only with the presence of a large amount of hydrogen and strain, and the peak was considered to be due to the interaction of dislocation with hydrogen.

The Bordoni peak and the peak at 220–280 K at 1 Hz appeared clearly for the α + β quenched specimen and the β quenched specimen. However, their peaks were difficult to occur for the β annealed specimen, because of the presence of β phase.

KEY WORDS: (Titanium Base Alloy) (Hydride) (Microstructure) (Internal Friction) (Transmission Electron Microscopy)

1. Introduction

α + β titanium alloys have been widely used for various structures in aerospace industries. Titanium alloys such as the Ti-6Al-4V can have numerous microstructures by means of heat treatment and welding process[1)–3)].

β annealed Ti-6Al-4V alloy which consisted of needle shaped α phase and β phase has a good fatigue strength[4)]. The fracture toughness of β quenched Ti-6Al-4V alloy consisted of α′ phase is higher than that of a mill annealed Ti-6Al-4V alloy consisted of α + β microstructure[5)].

The susceptibility to hydrogen induced cracking of their microstructures has been reported by Nelson et al.[6),7)], that is, hydrogen induced cracking occurs easily for α + β microstructure, and the role of hydride precipitation in hydrogen induced cracking is important factor.

The precipitation behavior of hydride has been reported by Boyd[8)], Hammond[9)], Enjo et al.[10)]. Hydrides precipitate in the α phase adjacent to α/β interface. But the hydride precipitation behavior on microstructure consisted of α′ phase, or α′ + α phase has not been clearly yet. α′ or α′ + α microstructure is usually recognized in the heat affected zone (HAZ) of welds.

Consequently, it is important to clarify the behavior of hydride precipitation of their microstructure in order to study the hydrogen induced cracking of HAZ of welds.

The purpose of this paper is to clear the precipitation behavior of hydrides in Ti-6Al-4V alloy with various microstructures cathodically charged at various current densities by using of X-ray diffraction technique, internal friction measurement and transmission electron microscopy.

2. Experimental Procedures

Ti-6Al-4V alloy plate was received in a mill annealed state. The thickness was 20 mm. The chemical compositions are shown in **Table 1**. The three kinds of thermal treatment was performed in a vacuum furnace. The temperature of the furnace was controlled to within ± 2 K.

The specimens were heated at 1278 K for 7.2 ks, and water quenched (β quenched specimen) or furnace cooled (β annealed specimen). And the specimen was heated at 1261 K for 7.2 ks, and water-quenched (α + β quenched specimen). And then α′, α + β and α′ + α microstructure were obtained.

Table 1 Chemical compositions of Ti-6Al-4V alloy (mass%).

Al	V	C	Fe	N	O	H	Ti
6.26	4.15	0.011	0.204	0.0042	0.146	0.0045	Bal

† Received on May 9, 1986

* Professor
** Research Instructor

Transactions of JWRI is published by Welding Research Institute of Osaka University, Ibaraki, Osaka 567, Japan

The hydrogen content was less than 10 ppm in all microstructures by vacuum gas analysis. The commercial pure titanium was also used. The material heat-treated was machined into specimens for X-ray diffraction technique and internal friction measurement (The size is 4 mm wide, 115 mm long and 0.8 mm thick).

The specimen surface was finished using aceton after the polishing by emery paper of number of 1500 before the tests.

Hydrogenation was carried out using cathodic charging method in a 5%H_2SO_4 aqueous solution. The cathodic charging was made at 4200 A/m^2, 500 A/m^2 and 50 A/m^2, in order to change the surface hydrogen concentration of the specimen.

X-ray line profiles were made by using X-ray diffractmeter with copper radiation filtered by Ni.

The internal friction measurement was performed using an inverted torsion pendulum over a temperature range of 70 K to 300 K at a frequency of about 1 Hz in the heating rate at 0.02 K/sec.

The specimens for transmission electron microscopy were prepared by jet polishing in the electrolyte consisted of 56 ml of perchloric acid, 230 ml of butyl alcohl, and 580 ml of methanol, after polishing up to 150 μm thick by emery paper of No. 1500. The electropolishing was performed at 14.5 V and below 233 K. The specimens were immediately examined in a Hitachi HU-12A electron microscope at 125 KV.

3. Results

3.1 Change in the internal friction curve by hydrogen charging.

Figure 1 shows photo and transmission electron micrographs, as the Ti-6Al-4V alloy was heat-treated variously.

For the β annealed Ti-6Al-4V alloy which was furnace-cooled from 1278 K, widmanstätten α phases are present in grain and α phase consists of packets[11] as shown in Fig. 1-(a), (b).

For the $\alpha + \beta$ quenched Ti-6Al-4V alloy which was water-quenched from 1261 K, α phase and α' phase around the α phase are present as shown in Fig. 1-(c), (d).

For the β quenched Ti-6Al-4V alloy which was water-quenched from 1278 K, the microstructure consists of α' phase, as shown in Fig. 1-(e), (f). Twin was also observed in the α' phase.

Figure 2 indicates internal friction versus temperature curves, as the β annealed Ti-6Al-4V alloy was cathodically charged at 4200 A/m^2 and 50 A/m^2 for various times.

For the internal friction curve at 4200 A/m^2, the peak at about 80 K is hydrogen Snoek relaxation peak in β phase, as shown in previous work[10]. The peak height increases with increasing hydrogen charging time, and saturates a certain value. For the internal friction curve at 50 A/m^2, the saturated value is lower than that at 4200 A/m^2, even though the hydrogen charging time is 86.4 ks.

For the internal friction curve at 4200 A/m^2, another peak generates at 190–220 K, which increases with increasing charging time, but the peak height at 50 A/m^2 is lower than that at 4200 A/m^2. This peak is due to the hydride precipitation as shown in previous work[10].

Figure 3 indicates internal friction versus temperature curves, as the $\alpha + \beta$ quenched Ti-6Al-4V alloy was cathodically charged at 4200 A/m^2 and 50 A/m^2 for various times.

For as-quenched condition, the peak is recognized at

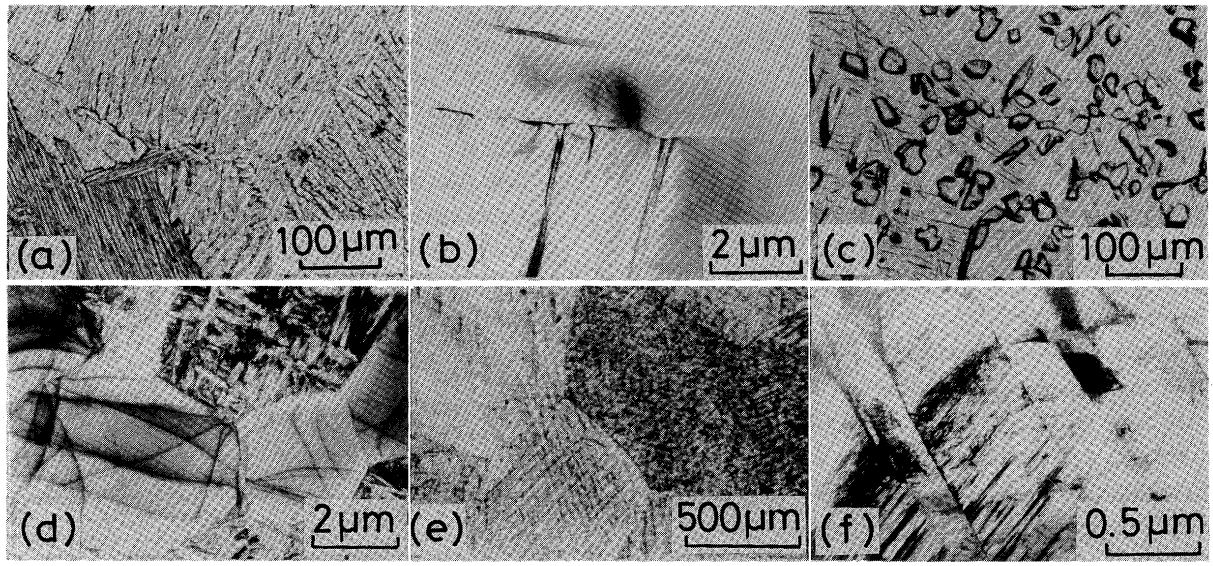

Fig. 1 Microstructures of Ti-6Al-4V alloy for β annealed specimen(a) and (b), $\alpha + \beta$ quenched specimen(c) and (d), and β quenched specimen(e), and (f).
(a), (c) and (e): Optical micrographs. (b), (d) and (f): Transmission electron micrographs.

120–200 K. The peak height increases and another peak generates at 240 K, as the charging time is 3.6 ks. For the hydrogenation at 14.4 ks, the peak at 110 K and the peak due to hydride precipitation at 190–220K are recognized, and another peak is clearly recognized at about 260 K. The hydrogen relaxation peak in the β phase is hardly recognized, though the peak is recognized for β annealed Ti-6Al-4V alloy shown in Fig. 2.

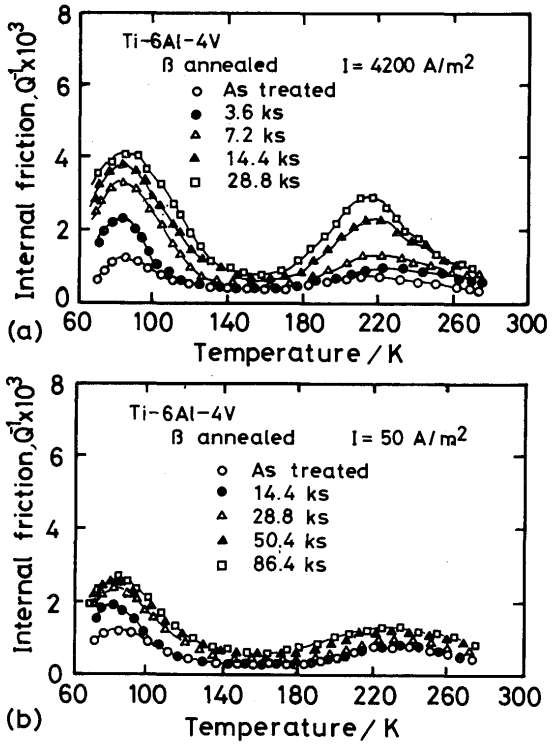

Fig. 2 Internal friction versus temperature curves for β annealed Ti-6Al-4V alloy cathodically charged at 4200 A/m² (a) and 50 A/m² (b) for various times.

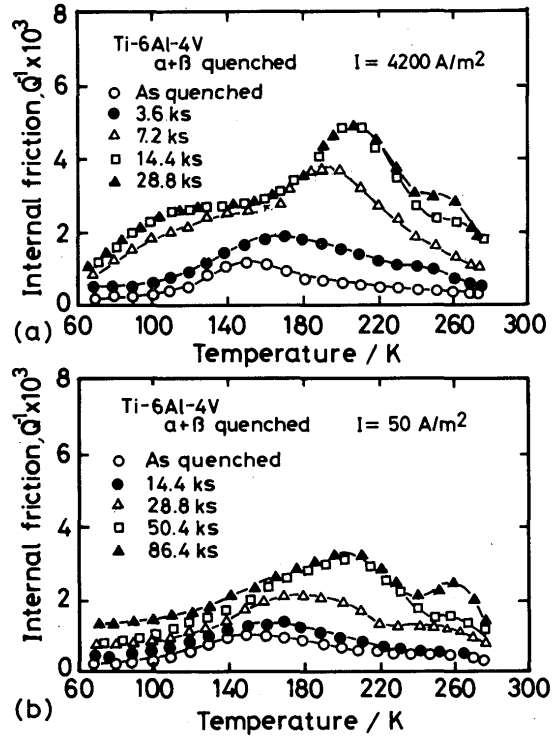

Fig. 3 Internal friction versus temperature curves for $\alpha + \beta$ quenched Ti-6Al-4V alloy cathodically charged at 4200 A/m² (a) and 50 A/m² (b) for various times.

The peak appeared in the temperature range of 80 K to 160 K increases with increasing hydrogen charging time. And the peak increases with increase in the amount of the hydride precipitation. For the charging time at 28.8 ks, the peak due to hydride precipitation at 190–220 K for the current density at 50 A/m² is lower than that at 4200 A/m².

Figure 4 indicates internal friction versus temperature curves, as the β quenched Ti-6Al-4V alloy was cathodically charged at 4200 A/m² and 50 A/m² for various times. For as-quenched condition, the peak generates at about 160 K. For the current density at 4200 A/m², the peak height at 120–200 K, at 190–220 K and at 250–280 K increases with increasing hydrogen charging time. These peaks hardly appears for the current density at 50 A/m².

Consequently, the peaks at 80–160 K, at 190–220 K and at 240–280 K are recognized in the internal friction curves of the $\alpha' + \alpha$ microstructure and α' microstructure. The internal friction curves are considered to be shown as the summary of these peaks, and the curves are fluent.

In order to evaluate the initiation mechanism of their peaks, the internal friction curves of commercially pure titanium consisting of the only α phase was investigated.

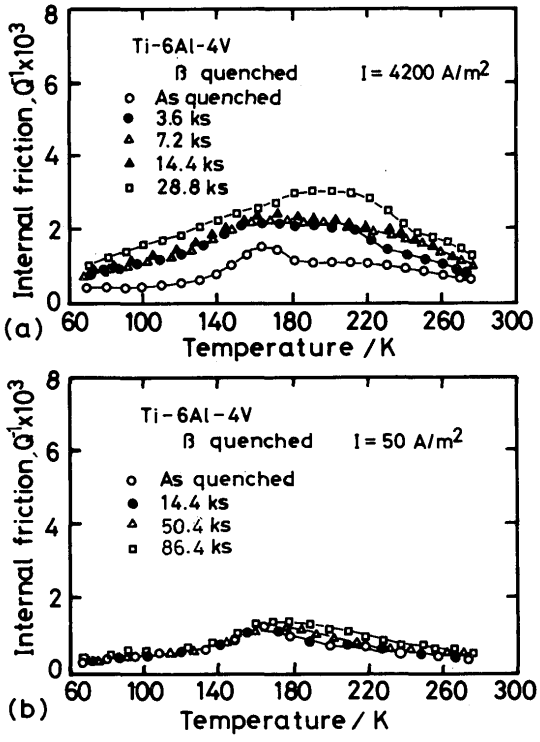

Fig. 4 Internal friction versus temperature curves for β quenched Ti-6Al-4V alloy cathodically charged at 4200 A/m² (a) and 50 A/m² (b) for various times.

Figure 5 indicates the internal friction curves, as the commercially pure titanium was annealed at 973 K for 3.6 ks in the vacuum furnace, and the plastically deformed for 2.8% and 6.5% at room temperature. For the annealed condition, the internal friction hardly changes over a wide range of temperature from 70 K to 280 K. But as the annealed commercially pure titanium was plastically deformed, a peak generates at 120–220 K, and the peak height increases with increase in the amount of plastic deformation. This peak is considered to be Bordoni peak generated due to plastic deformation in α phase.[13)–15)]

Consequently, the peak at 120–200 K for Ti-6Al-4V alloy shown in Fig. 3 and Fig. 4 is considered to be Bordoni peak in α phase.

Figure 6 indicates the internal friction versus temperature curves, as the commercially pure titanium was cathodically charged at 500 A/m^2 for 50.4 ks and then plastically deformed. The peak due to hydride precipitation generates at 190–220 K by hydrogenation. For the commercially pure titanium plastically deformed after hydrogenation, Bordoni peak appears at 110–180 K, and the peak due to hydride precipitation at 190–220 K become higher. A new peak appears at 240–280 K, which is generated by both hydrogenation and the existence of the deformation. This peak is also detected for Ti-6Al-4V alloy consisted of $\alpha' + \alpha$ microstructure.

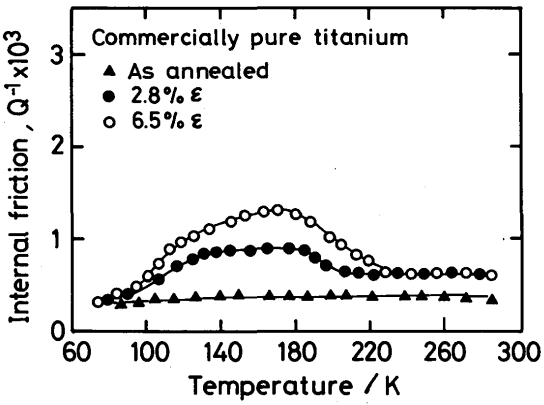

Fig. 5 Internal friction versus temperature curves for commercially pure titanium annealed and plastically deformed.

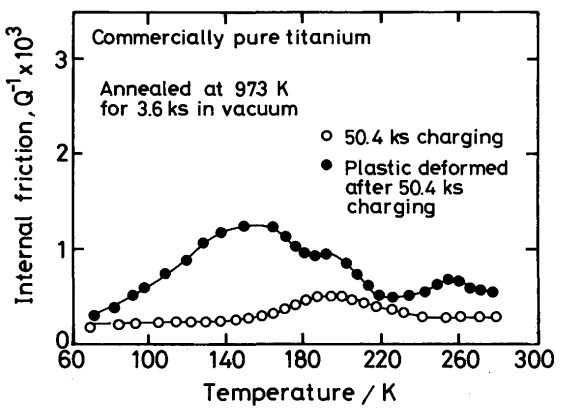

Fig. 6 Internal friction versus temperature curves for commercially pure titanium cathodically charged at 500 A/m^2 for 50.4 ks and then plastically deformed.

Figure 7 indicates the internal friction versus temperature curves for commercially pure titanium thermally hydrogenated under various hydrogen partial pressures for 7.2 ks and furnace cooled. Bordoni peak at 100–160 K, the peak due to hydride precipitation at 180–220 K and the peak at 240–280 K are detected. The height of peak due to hydride precipitation at 180–220 K increases with increasing hydrogen partial pressure. Then, the hydride precipitation behavior in the commercially pure titanium was also discussed.

Figure 8 shows optical micrographs for the commercially pure titanium cathodically charged at 500 A/m^2 for 50.4 ks(a) and thermally hydrogenated under 0.05 MPaH_2 for 7.2 ks(b). The hydride precipitation in their samples was also detected by using X-ray diffraction technique. For cathodic charging, the hydride precipitates at the grain boundary, but the hydride precipitates at α/α interface for thermally hydrogenated sample.

3.2 Hydride precipitation in various microstructures.

Figure 9 indicates the surface morphology by SEM of the β annealed Ti-6Al-4V alloy cathodically charged at 4200 A/m^2 for 28.8 ks. The surface before charging is very flat as shown in Fig. 9-(a). The surface after charging indicates the presence of white band in α phase or at α/β interface, and the white band was also observed as a needle shaped line in the α phase. By means of stereo-matching techniques, the bands are clear to be swelled. This is considered to have been swelled due to hydride precipitation. The amount of swell was fewer at the small current density.

Figure 10 shows a transmission electron micrograph for the β annealed Ti-6Al-4V alloy cathodically charged at

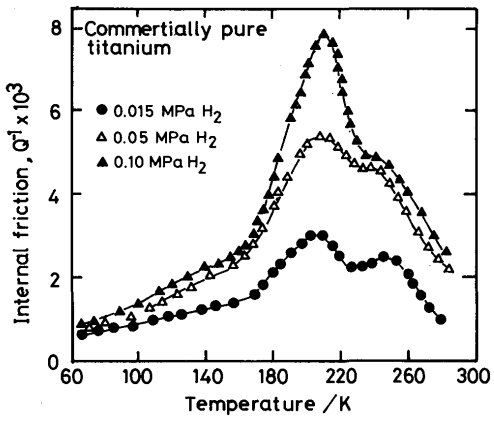

Fig. 7 Internal friction versus temperature curves for commercially pure titanium thermally hydrogenated under various hydrogen partial pressures for 7.2 ks and then furnace-cooled.

4200 A/m^2 for 14.4 ks. The strain contrast due to hydride precipitation was observed in the α phase at α/β interface. The granular precipitates are also observed in the β phase. These precipitates were identified as γ hydride by means of selected area diffraction pattern. The hydrides precipitate in the α phase from α/β interface, and strain contrast around the hydrides is recognized. This phenomena corresponds the white needle shaped lines shown in Fig. 9. For the current density at 50 A/m^2, the hydrides hardly precipitate in the α phase, but precipitate only at α/β interface.

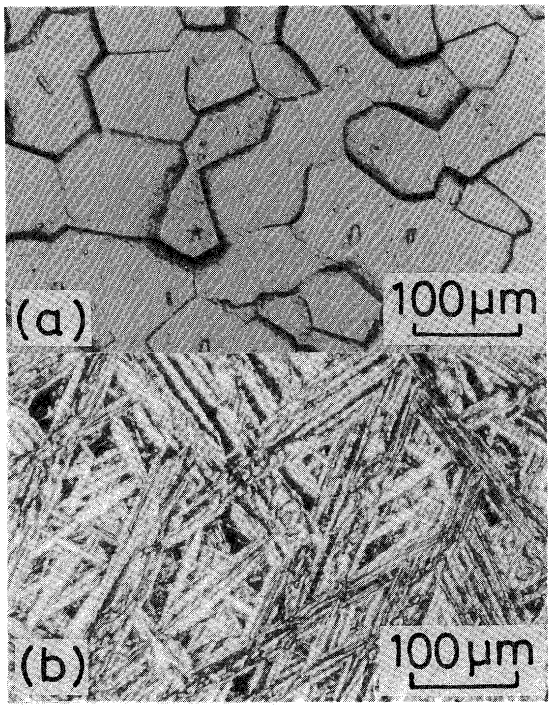

Fig. 8 Optical micrographs for commercially pure titanium cathodically charged at 500 A/m^2 for 50.4 ks (a) and thermally hydrogenated under 0.05 MPa H_2 for 7.2 ks (b).

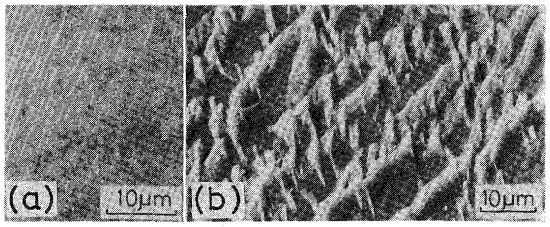

Fig. 9 Surface morphology of β annealed Ti-6Al-4V alloy cathodically charged at 4200 A/m^2 for 28.8 ks.
(a): Before charging. (b): After charging.

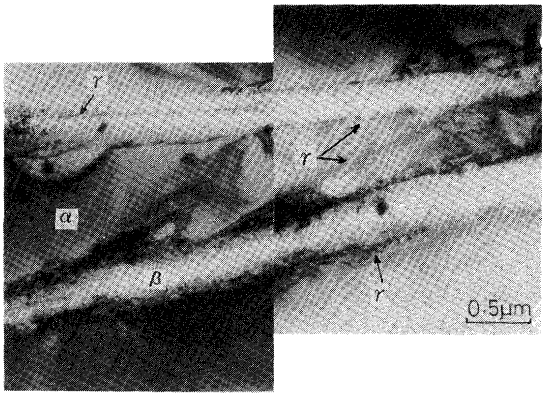

Fig. 10 Transmission electron micrograph for β annealed Ti-6Al-4V alloy cathodically charged at 4200 A/m^2 for 14.4 ks.

Figure 11 shows transmission electron micrographs, as the $\alpha+\beta$ quenched Ti-6Al-4V alloy was cathodically charged at 4200 A/m^2 for 14.4 ks. The hydrides are recognized as darkend area precipitate in the primary α phase at α'/α interface, which produced strain contrast.

Figure 12 shows transmission electron micrographs near the surface of the sample, as the β quenched Ti-6Al-4V alloy was cathodically charged at 4200 A/m^2. As shown in Fig. 12-(a), α' phase is considerably deformed by the hydride precipitation, which is suggested by bend contour. Selected area diffraction patterns around the circle is shown in Fig. 12-(c). In this pattern, it was confirmed the presence of γ hydride phase of fcc structure precipitated in the orientation relationship $(001)_{\alpha'}$//

Fig. 11 Transmission electron micrograph for $\alpha+\beta$ quenched Ti-6Al-4V alloy cathodically charged at 4200 A/m^2 for 14.4 ks.

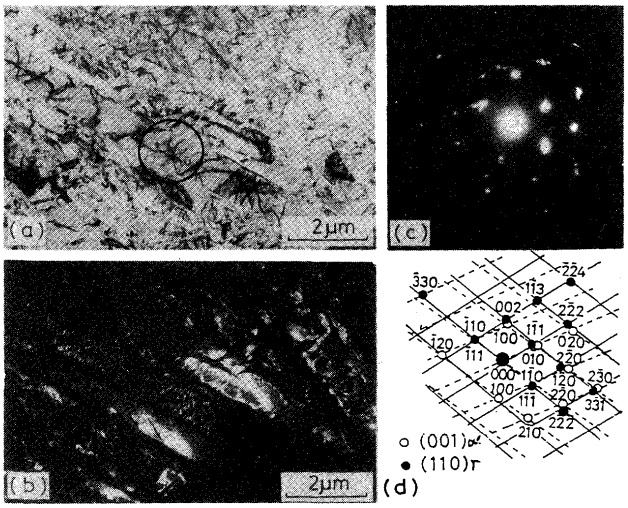

Fig. 12 Transmission electron micrographs for β quenched Ti-6Al-4V alloy cathodically charged at 4200 A/m^2 for 14.4 ks.
(a): Bright field image, (b): Dark field image, (c) and (d): Diffraction pattern.

$(110)_\gamma$. Dark field image from $2\bar{2}2_\gamma$ spot in shown in Fig. 12-(b). The hydrides precipitate in the α' lath and at α'/α' interface.

Figure 13 shows transmission electron micrographs of inner area of the sample, as the β quenched Ti-6Al-4V alloy was cathodically hydrogen-charged at 4200 A/m^2 for 14.4 ks. Darkened phases are recognized at α'/α' interface, and this phase is hardly observed before charging, as shown in Fig. 1-(f). Consequently, this phase is considered to be γ hydrides. The lath shaped α' phase is considerably deformed by the hydride precipitation, and the lath is recognized as granular shape owing to bend contour.

Then, X-ray diffraction profiles were also measured. The profiles of the β annealed Ti-6Al-4V alloy were similar to that of mill annealed Ti-6Al-4V alloy in previous work[10]. Namely, the peaks of α phase and β phase were recognized before hydrogen charging, and the peak due to hydride precipitation was recognized at 60.9° after hydrogen charging. However, the hydride precipitation was hardly detected even though the charging time becomes longer such as 50.4 ks for the $\alpha + \beta$ quenched Ti-6Al-4V alloy and the β quenched Ti-6Al-4V alloy.

4. Discussion

4.1 Hydride precipitation behavior

For $\alpha + \beta$ Ti alloy, hydrides of several crystal structures have been reported in ASTM cards (9-371, 25-982, 25-983). By means of transmission electron microscopy, only γ hydride of fcc structure can be detected, and the lattice parameter is a = 0.44 nm or a = 0.433 nm[8),16)]. For Ti-8Al-1Mo-1V alloy, the orientation relationship is reported as $\{0001\}_\gamma // \{001\}_\gamma, \{0001\}_\alpha // \{112\}_\gamma, \{001\}_\alpha // \{110\}_\gamma$ according to Boyd[8)] and $(10\bar{1}0)_\gamma // (101)_\gamma$, $[1120]_\alpha // [011]_\gamma$ according to Blackburn[17)].

For Ti-5Al-2.5 Sn alloy, the relationship is reported as $(001)_\alpha // (111)_\gamma$, $\langle 1210\rangle_\alpha // \langle 1\bar{1}0\rangle_\gamma$ according to Hammond[4)] and $(0001)_\alpha // (001)_\gamma$, $\langle 1\bar{2}10\rangle_\alpha // \langle 1\bar{1}0\rangle_\gamma$ according to Hall[16)].

For Ti-6Al-4V alloy, Pittinato[2)] and Hoeg et al.[8)] observed fcc γ hydride phase in thermally hydrogenated sample. In present investigation, hydride phase was also observed as same as the result by Boyd[8)] in the hydrogenation by cathodic charging. Furthermore, a ribbon-type[19)], and A-type and B-type[9),16)]-hydrides were also observed partially, but their crystal structure has not been known yet.

For α' microstructure or $\alpha' + \alpha$ microstructure shown in Fig. 12 and Fig. 13, hydrides precipitate in the α' phase and at α'/α' interface, and the crystal structure was $(0001)_{\alpha'} // (110)_\gamma$, $\langle 1210\rangle_{\alpha'} // \langle 110\rangle_\gamma$. This result corresponds to the results in α phase by Boyd[8)].

For the hydrogenation by cathodic charging to the $\alpha + \beta$ microstructure, hydrogen is absorbed to the β phase, and diffuses to inner area of the specimen through the β phase, because the solubility and diffusivity of hydrogen in β phase are far higher than those in α phase. It is considered that hydrogen atoms diffuse not only in the α phase near the specimen surface but also in the α phase at α/β interface inside the specimen, as shown in the models of Fisher[19)] and Whipple[20)]. As the results, the hydrides are considered to precipitate in the α phase.

Recently, it is reported that a interface phase precipitates at α/β interface during slow cooling for β annealed Ti-6Al-4V alloy[21)]. But it is also reported that the interface phase is artifact pattern revealed during electrolytic polishing[22)]. In present investigation, the interface phase was hardly observed for the β annealed Ti-6Al-4V alloy.

For the hydrogenation by cathodic charging to α' microstructure and $\alpha' + \alpha$ microstructure, the γ hydrides precipitated in the α' phase and at α'/α' interface were observed in the area near the specimen surface as shown in Fig. 12. It is considered that the hydrides precipitated at α'/α' interface as shown in Fig. 13, because the hydrogen atoms diffuse through α'/α' interface in the inner side of the specimen.

The hydrides could be hardly detected by using X-ray diffraction technique, and it means that the hydrides precipitate as a very thin layer only near the specimen surface.

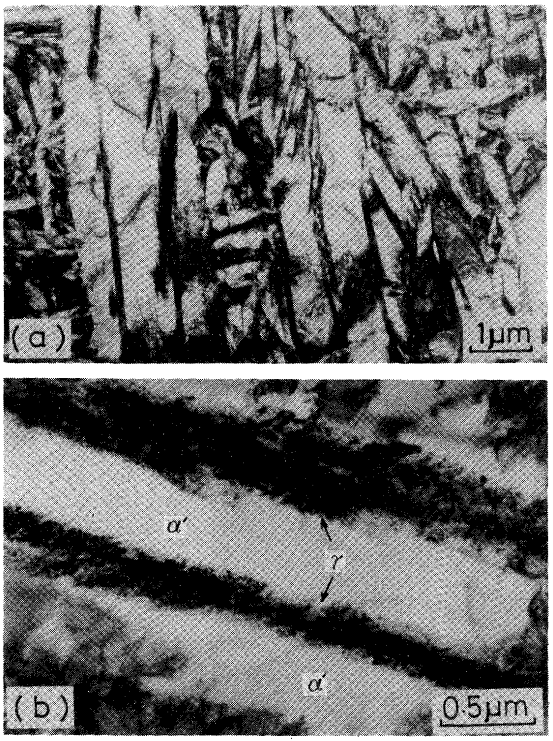

Fig. 13 Transmission electron micrographs for β quenched Ti-6Al-4V alloy cathodically charged at 4200 A/m^2 for 14.4 ks.

4.2 The mechanism of internal friction by hydrogenation

In this section, the mechanism of internal friction peak due to hydrogenation for various microstructure, and the effect of hydride precipitation on the deformation of matrix and discussed.

For the commercially pure titanium, the peak generates at about 190 K in the internal friction versus temperature curve for 50.4 ks hydrogen charging, as shown in Fig. 6.

The specimen was also measured by X-ray diffraction technique. As a result, the peak of γ hydride phase appeared at 59°, 71°, and 74° in the diffraction angle (2θ), as same as described by ASTM cards. Consequently, the internal friction peak at 190 K is considered to be reliable to associate to hydride precipitation as shown in previous work[10].

As shown in Fig. 7, two kinds of peak in the internal friction versus temperature curve of the specimen were observed, as the commercially pure titanium was thermally hydrogenated at 1273 K, and then furnace-cooled. The peak height at about 190 K increases with increasing hydrogen partial pressure.

As shown in Fig. 8, hydrides precipitated at α/α interface. Consequently, it is considered that the peak at about 190 K for Ti-6Al-4V alloy shown in Fig. 3 is not due to hydrogen relaxation peak in α phase, but is due to stress induced diffusion in the hydride[10].

As shown in Fig. 3, the peak at 110–160 K increases with increase in the peak due to hydride precipitation at 190–210 K. This peak is considered to be Bordoni peak.

As shown in Fig. 11 and Fig. 12, the precipitation of the hydride causes the deformation of the α' phase and the α phase. And the amount of deformation in α' phase and α phase increases with increasing the amount of hydrides. Consequently, the Bordoni peak becomes high.

As shown in Fig. 2, the Bordoni peak at 110–200 K hardly generates for $\alpha+\beta$ microstructure, and it is considered that β phase relaxed the deformation of α phase[25].

In Fig. 7, Someno et al.[26] reported that the peak at 220–280 K in the internal friction versus temperature curve is due to the stress induced diffusion in the titanium hydride. However, as shown in Fig. 6, the peak hardly generates, as the commercially pure titanium was hydrogenated by cathodic charging. And the peak generates at 220–280 K in the internal friction versus temperature curve, as the commercially pure titanium was hydrogenated by cathodic charging and then plastically deformed. The phenomena appears for $\alpha'+\alpha$ Ti-6Al-4V alloy and α' Ti-6Al-4V alloy, as shown in Fig. 3.

On the basis of Fig. 3 and Fig. 4, the peak at 260 K generates due to both the existence of a large amount of hydrides and the presence of Bordoni peak.

According to Fig. 10 and Fig. 12, the α phase around the hydride was deformed. This result is also proposed by Williams[27]. Consequently, the mechanism of the peak at 260 K is considered to be hydrogen and dislocation interaction[13),28].

5. Conclusion

Effect of the microstructure on the hydride precipitation behavior has been studied on a Ti-6Al-4V alloy cathodically charged at various current densities using internal friction measurement and transmission electron microscopy.

The results obtained in this investigation are summarized as follows.

1) The hydride precipitation by cathodic hydrogen-charging was observed not only near the surface but also inside the specimen for the β annealed Ti-6Al-4V alloy consisting of $\alpha+\beta$ microstructure. But the hydride precipitation was observed only near the surface of the specimen for the β quenched Ti-6Al-4V alloy of α' microstructure, and for the $\alpha+\beta$ quenched Ti-6Al-4V alloy consisting of $\alpha'+\alpha$ microstructure.
2) For the β annealed Ti-6Al-4V alloy, the absorption of hydrogen in the β phase can be detected by the peak at 80 K in the internal friction versus temperature curve. The peak associated hydride precipitation at 180–220 K can be detected, and the peak height increased with increasing the current density. The hydrides precipitate in the α phase and at α/β interface. Furthermore, the hydrides precipitate not only in the α phase but also in the β phase for the high current density.
3) For the $\alpha+\beta$ quenched Ti-6Al-4V alloy, the peak associated hydride precipitation at 180–220 K in the internal friction versus temperature curve increases with increasing cathodic hydrogen-charging time. The peak at 220–280 K increases with increase of the peak height at 180–220 K. The hydrides precipitate in the α phase adjacent to α'/α interface and at the α'/α' interface.
4) For the β quenched Ti-6Al-4V alloy, the hydride can be hardly detected by means of X-ray diffraction technique, but can be detected by the internal friction measurement. Hydrides precipitate at α'/α' interface and grew into the α' phase. The deformation of the matrix due to the hydride precipitation was observed by means of the strain contrast around the hydride by transmission electron microscopy.
5) On the basis of the internal friction measurement and transmission electron microscopy, the hydride precipitation causes the Bordoni peak, because of the deformation of the matrix. The peak at 220–280 K appears

by the presence of a large amount of hydrogen and strain, and the peak was considered to be due to the interaction of dislocation with hydrogen. The Bordoni peak and the peak at 220–280 K appeared clearly for the $\alpha + \beta$ quenched Ti-6Al-4V alloy and the β quenched Ti-6Al-4V alloy. However, their peaks were difficult to occur for the β annealed Ti-6Al-4V alloy, because of the presence of the β phase.

Acknowledgement

The authors wish to thank Mr. T. Imataka for his variable contribution in this work.

References

1) W.A. Baeslack and C.M. Banas: Weld. J., (1981), 121s.
2) R.E. Lewis and K.C. Wu: Weld. J., (1963), 241s.
3) M.A. Imam and C.M. Gilmore: Metall. Trans. A, 14A, (1983), 233.
4) G.R. Yoder, L.A. Cooley and T.W. Crooker: Metall. Trans. A. 8A, (1977), 1737.
5) I.W. Hall and C. Hammond: Titanium Sci. Technol., Proc. Int. Conf.-, 2nd, Plenum Press, New York, (1972), 1365.
6) H.G. Nelson, D.P. Williams and J.E. Stein: Metall. Trans., 3, (1972), 1972.
7) H.G. Nelson: Metall. Trans., 4, (1973), 364.
8) J.D. Boyd: ASTM (Amer. Soc. Metals), Trans. Quart., 62, (1969), 977.
9) C. Hammond, R.A. Spurling and N.E. Paton: Metall. Trans. A, 15A, (1984), 813.
10) T. Enjo and T. Kuroda: Nippon kinzoku gakkaishi, 49, (1985), 320 (In Japanese).
11) D. Eylon: Metall. Trans., A, 10A, (1979), 311.
12) G.F. Pittinato and W.D. Hanna: Metall. Trans., 3, (1972), 2905.
13) R.R. Hashiguti, N. Igata and G. Kamoshita: Acta Metall., 10, (1962) 442.
14) L.T. Miyada, S. Watanabe, K. Kamoshita and A. Isore: Internal friction and Ultrasonic Attenuation in Solids, Proc. Int. Conf., Univ. of Tokyo Press, (1977), 605, Tokyo, Jpn.
15) A. Seeger: Phil. Mag., 1, (1956), 651.
16) I.W. Hall: Metall. Trans., A, 9A, (1978), 815.
17) M.J. Blackburn: Trans. ASM, 59, (1966), 694.
18) H. Hoeg, B. Hollund and I.W. Hall: Met. Sci., 14, (2), (1980), 50.
19) J.C. Fisher: J. Appl. Phys., 22, (1951), 74.
20) R.T. Whipple: Phil. Mag., 45, (1954), 1255.
21) C.G. Rhodes and N.E. Paton: Metall. Trans., A, 10A, (1979), 209.
22) J.E. Costa, D, Banerjee and J.C. Williams: Beta Titanium Alloys in the 80's, Int. Conf. of Metall. Soc. AIME, (1983), Atranta, USA.
23) D.J. Ju: J. Phys. Colloq., C5-Pt. 2, (1981), 775.
24) O. Buck, D.O. Thompson and C.A. Wert: J. Phys. Chem. Solids, 34, (1973), 591.
25) T. Enjo and T. Kuroda: Hydrogene Mater., Cong., Int., 3rd, 1, (1982) 161, Paris, Fr.
26) D. Someno, H. Nagasaki and Y. Miyasaka: Nippon kinzoku gakkaishi, 31, (1967), 957, (In Japanese).
27) J.C. Williams: Eff. Hydrogen Behav. Mater., Proc. Int. Conf., (1975), 367, USA.
28) P.P. Tung and A.W. Sommer: Acta Metall., 22, (1974), 191.